

23 March 2022

# Growth and superconducting transition of $\text{Pr}_{1-x}\text{Ca}_x\text{Ba}_2\text{Cu}_3\text{O}_{7-\delta}$ ( $x \approx 0.5$ ) epitaxial thin films

J. Y. Xiang, Z. Y. Liu, J. Li, P. Wang, R. L. Wang, H. P. Yang, Y. Z. Zhang, D. N. Zheng<sup>§</sup>, H. H. Wen, and Z. X. Zhao

National Laboratory for Superconductivity, Institute of Physics and Center for Condensed Matter Physics, Chinese Academy of Sciences, Beijing 100080, People's Republic of China.

**Abstract.**  $\text{Pr}_{1-x}\text{Ca}_x\text{Ba}_2\text{Cu}_3\text{O}_{7-\delta}$  ( $x \approx 0.5$ ) thin films have been grown on  $\text{SrTiO}_3$  and YSZ substrates by the pulsed laser ablation. The substrate temperature dependence of orientation and superconducting properties were systematically studied. Good quality  $c$  and  $a$ -axis orientated films can be obtained on  $\text{SrTiO}_3$  via changing the substrate temperature solely. On YSZ, films with good  $c$ -axis orientation can be grown, while it is hard to grow films with good  $a$ -axis orientation by changing substrate temperature alone. The highest  $T_{C0}$  is about 37K, which is found in the films grown on YSZ with a good  $c$ -axis orientation. For the films grown on STO, however, the highest  $T_{C0}$  is about 35.6K with a mixed orientation of  $c$ -axis and  $a$ -axis. In most of the superconducting films, the weak temperature dependence of the normal state resistivity, as characterized by small  $R(290\text{K})/R(50\text{K}) \leq 2$  ratios, together with a weak localization behavior just above  $T_C$  could be attributed to the essential scattering due to the localized electronic states. The superconducting transitions in a field up to 10 T along  $c$ -axis have been measured on a  $c$ -axis oriented film grown on  $\text{SrTiO}_3$ . The zero-temperature in-plane upper critical field  $B_{C2}^{ab}(0)$  is estimated from the resistivity transition data.

PACS numbers: 81.15.Gh, 68.55.-a, 74.78.Bz, 74.72.-h

Submitted to: *Supercond. Sci. Technol.*

<sup>§</sup> To whom correspondence should be addressed (e-mail: Dzheng@ssc.iphy.ac.cn)

## 1. Introduction

Among the high  $T_C$  cuprates, compounds with  $RBa_2Cu_3O_{7-\delta}$  ( $R$ =rare-earth elements) structure, the so-called 123 structure, have properties which are nearly independent of  $R$  except for  $R=Pr$ [1, 2]. Although  $PrBa_2Cu_3O_{7-\delta}$  (*Pr-123*) can be formed, it does not show superconductivity at low temperature and even shows no metallic behavior[3]. There are also reports on superconductivity in *Pr-123*[4, 5], however, the bulk superconductivity of *Pr-123*, has to be independently verified and also the structure of superconducting *Pr-123* has to be confirmed by rigorous crystallography. Optical study has shown that  $PrBa_2Cu_3O_{7-\delta}$  is a charge transfer type insulator with a charge-transfer gap  $\Delta_{CT} \sim 1.4$  eV, and carriers in the chain are localized at low temperatures and low frequencies [6]. Due to the depletion of mobile carriers, the in-plane electric transport properties in *Pr-123* could be described in terms of variable range hopping (VRH) in the insulating region [7]. When the high-temperature cuprates are doped with *Pr* the superconductivity is usually suppressed [8], and often a metal-insulator transition occurs, accompanied by the presence of complicated magnetic behavior due to the relatively large magnetic moment of *Pr* ions [9]. The origin of the suppression of superconductivity in HTSC by *Pr* and absence of superconductivity in *Pr-123*, being of fundamental interest, may also shed light on the mechanism of high-temperature superconductivity, since any reasonable theory should explain the effect of *Pr* on superconductivity in 123 systems.

If the carriers depletion were indeed the main origin for the absence of superconductivity in *Pr-123*, a simple approach could be to introduce carriers by chemical doping. A substitution of divalent element such as Ca for *Pr* appears to be a natural choice. Nevertheless no superconductivity was found in the samples with fairly low Ca doping levels (less than 30% at ambient pressure[10, 11]). Norton *et al.* successfully revived superconductivity in *Pr-123* epitaxial thin films by substituting 50% of the tetravalent *Pr* by divalent Ca [12, 13]. And later, superconductivity was again found in high-pressure synthesized Ca-doped *Pr-123* bulk samples [14, 15]. However, the influence of crystal structures on superconductivity in the thin films is still somewhat ambiguous. For example, it is necessary to study the superconductivity in films with different orientations systematically. And also it is important to make a comparative study of the transport properties of thin films and that of ceramic bulk samples. The transport properties of Ca-doped *Pr-123* bulk samples sintered at ambient pressure have been studied by Luszczek [16]. However, researches are harassed by the limited Ca substitution levels and no superconductivity was observed. Whereas, for the samples synthesized at high pressures, impurity phases seems hard to be avoided, although the Ca content is highly improved [17]. In this article, we report a systematical investigation on the substrate temperature dependence of film orientation, the superconducting transition temperature and the residual-resistivity ratio for  $Pr_{0.5}Ca_{0.5}Ba_2Cu_3O_{7-\delta}$  thin films grown on the substrates of  $SrTiO_3$  and Yttrium-stabilized  $ZrO_2$ . The superconducting transition data of  $Pr_{0.5}Ca_{0.5}Ba_2Cu_3O_{7-\delta}$

epitaxial thin films measured in a magnetic field up to 10 T, applied parallel to  $c$ -axis of the films, are analyzed.

## 2. Film growth and characterization

A  $Pr_{0.5}Ca_{0.5}Ba_2Cu_3O_{7-\delta}$  ceramic target was prepared using a conventional solid state reaction method similar to that used to produce superconducting R-123 pellets. The stoichiometric quantities of high-purity dry  $Pr_6O_{11}$ ,  $CaCO_3$ ,  $BaCO_3$ , and  $CuO$  powders were ground, mixed, fired, pelletized and sintered for several times. The sintering temperature was 930 °C. The whole process was carried out in air under an ambient pressure. Powder X-ray diffraction indicated a predominant R-123 phase while a small amount of  $BaCuO_2$  could also be detected. The  $Pr_{0.5}Ca_{0.5}Ba_2Cu_3O_{7-\delta}$  epitaxial thin films were grown using pulsed-laser ablation mainly on the substrates of  $SrTiO_3$  (STO) and Yttrium-stabilized  $ZrO_2$  (YSZ). Some  $LaAlO_3$  (LAO) and  $(LaAlO_3)_{0.3} - (Sr_2AlTaO_8)_{0.7}$  (LSAT) substrates were also used. A silicon heater was utilized in the film deposition, and the temperature was monitored by an infrared thermodetector with a calibrated temperature range from 300 °C to 1200 °C. A self-made NiCr-NiAl thermocouple was placed at the back of the heater as a temperature reference. A LPX 300 KrF ( $\lambda = 248$  nm) excimer laser (Lambda Physik) was adopted for the film growth. The repetition rate was 5 Hz and the fluence was about 2 J/cm<sup>2</sup>. The target-substrate distance was kept at 70 mm. The films were deposited in an oxygen partial pressure of 40 Pa, as frequently seen in the growth of YBCO. After deposition, a one-minute holding before annealing was used for the purpose of stress relaxation. The annealing process was carried out in 1 atm oxygen at a cooling rate around 15 °C/min for about 10 minutes (The superconductivity of the film was found hardly dependent on the annealing duration at this circumstance). The films were then cooled down naturally to room temperature. The superconducting critical temperature of the films was measured using a standard four-probe technique, with the electrodes mounted by silver paste on the films directly.

Inductively coupled plasma (ICP) results show a good consistency of the film stoichiometry with that of the target, as expected from the pulsed-laser ablation method. The orientation of the films was characterized by X-ray diffraction (XRD). On STO, films with  $c$ -axis lying in the film plane ( $a$ -axis oriented) can be obtained by decreasing the substrate temperature  $T_S$  for about 160 °C, as compared with that for films with  $c$ -axis perpendicular to the film surface ( $c$ -axis oriented). Typical XRD patterns for films with  $c$  and  $a$ -axis orientation, grown at a temperature of 880 °C and 720 °C, are shown in Fig. 1a and Fig. 1c, respectively. Films grown at an intermediate  $T_S$  of  $\sim 740$  °C possess a structure with mixed  $c$  and  $a$ -axis orientated phases, as shown in Fig. 1b. A weak (103) peak, which is the strongest line of the target spectrum, can sometimes be seen as  $T_S$  was further reduced. The surface profile of the films were obtained by atomic force microscopy (AFM). The mean roughness is around 4 nm and 20 nm in a  $10 \times 10 \mu m^2$  area for the  $a$  and  $c$ -axis oriented films, respectively. As a

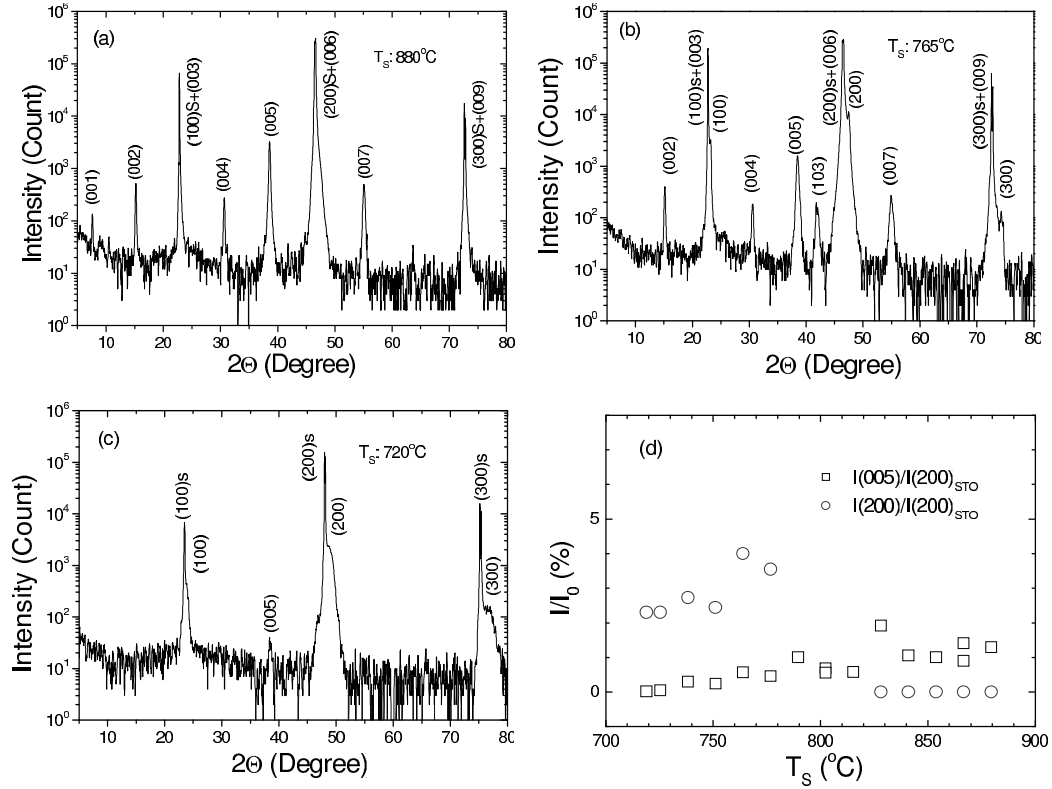


**Figure 1.** Influence of the substrate temperature  $T_S$  on the orientation of  $\text{Pr}_{0.5}\text{Ca}_{0.5}\text{Ba}_2\text{Cu}_3\text{O}_{7-\delta}$  thin films grown on STO. Typical XRD patterns for films grown at  $T_S$  of (a) 880 °C, (b) 765 °C, and (c) 720 °C are shown. Peaks of the substrate are marked with a postfix "s". Shown in (d) is the  $T_S$  dependence of the ratio  $I(005)/I(200)_S$  and  $I(200)/I(200)_S$ , where  $I(hkl)$  is the diffraction intensity of  $(hkl)$  peak for the film or the substrate.

comparison, the intensity ratios of (005) and (200) of the film to (200) of the substrate, varying with  $T_S$ , are also shown in Fig. 1d. Typical resistance transitions for the films with different orientation are shown in Fig. 2. Here, the resistance of the films scaled by the respective value at 290 K,  $R(290\text{K})$ . Label 'c-oriented', 'mixed oriented' and 'a-oriented' of the curves corresponds to a substrate temperature of 880 °C, 790 °C and 720 °C, respectively. The low temperature part of transition of the curves are also zoomed in the inset of Fig. 2 for a clearer view. It is evident that the film structure has a substantial effect on both superconducting and normal state properties of the film. On YSZ substrates, good quality *c*-axis oriented films can also be obtained, as shown in Fig. 3. The substrate temperature in such a growth process was around 900 °C, slightly higher than that in the case of STO. It can be attributed to the 45 ° rotation of the  $R-123$  unit cells on YSZ. However, it was found difficult to grow *a*-axis films on YSZ solely by varying  $T_S$ . When  $T_S$  was reduced lower than that for *a*-axis oriented films grown on STO, more and more characterized peaks of the target appeared. A typical XRD pattern for the films grown at about 700 °C is shown in Fig. 3b. We can see that

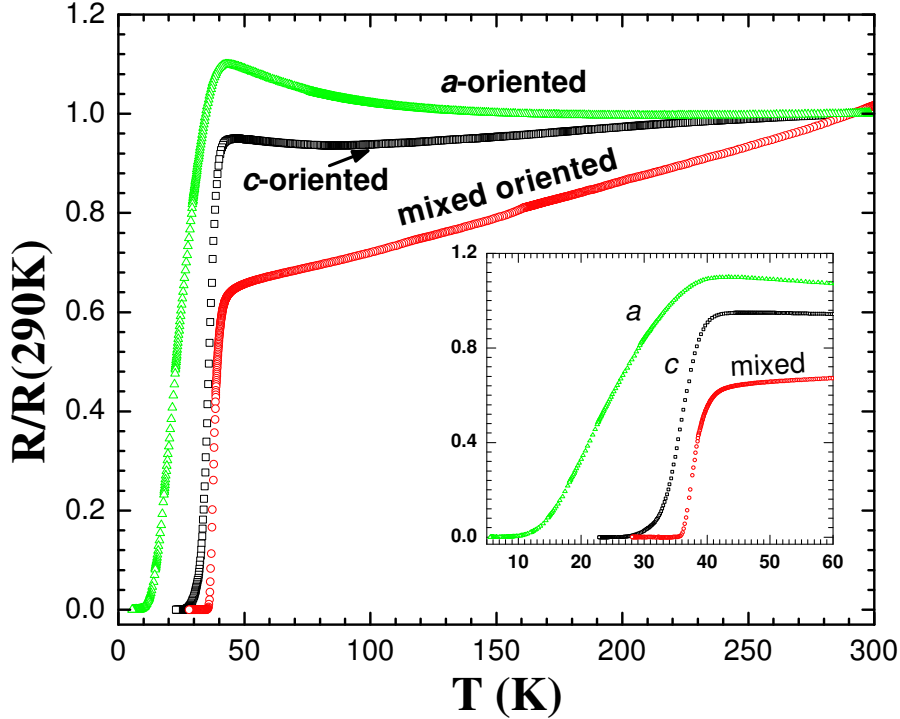


**Figure 2.** Typical resistance transition of different oriented films grown on STO. The resistance of these films are normalized to the value at 290 K, *i.e.*,  $R(290\text{K})$ . Here, labels with 'c-oriented', 'mixed oriented' and 'a-oriented' correspond to a substrate temperature of 880 °C, 790 °C and 720 °C, respectively. Inset is the low temperature part of the transition of these films.

peaks other than the (00 $l$ ) and ( $l$ 00) are shown. For substrates such as LAO and LSAT, good quality  $c$ -axis oriented films can also be obtained.

It is found that the critical temperature changes with the substrate temperature. Fig. 4 shows the substrate temperature  $T_S$  dependence of the critical temperature for films grown on STO. The error bar of  $T_{C\text{onset}}$  and  $T_{C0}$  corresponds to the temperature scope from 100% to 90% of  $\rho_n$ , and 10% to 0 (within the resolution of the instruments used) of  $\rho_n$ , respectively. Here  $\rho_n$  is the normal state resistivity, defined as the value where the sample resistivity deviates from the linear temperature dependence near the superconducting transition. The relationship of  $T_C$  and  $T_S$  for the films on YSZ is also shown. A higher  $T_S$  is necessary to grow epitaxial thin films on YSZ than on STO, due to the larger lattice mismatch of the former. Accordingly,  $T_C$  for the films on YSZ is higher, which could also be due to a larger strain at the interface. The highest  $T_{C0}$  is about 35.6 K and 37 K for the films grown on STO and on YSZ, respectively. It is worthy to notice that on STO, films with higher  $T_{C0}$  are those with a structure of mixed  $c$ -axis and  $a$ -axis oriented phases, as was reported earlier by Norton *et al.* [12]. For the

films grown on YSZ, the variation tendency of the measurement data seem to suggest a better superconductivity for the  $c$ -axis oriented films than those with  $a$ -axis orientation.

An interesting thing of the films is their metastable properties. As the solubility of Ca in the bulk materials sintered at ambient pressure is less than 30%, metastable properties of the target with higher Ca doping levels could be expected, as having been pointed out by Norton *et al.* [13]. Sintering the bulk materials under high pressure can raise the Ca substitution level to 70%. Superconductivity exhibits in bulks with Ca doping level from 30% to 70%, as mentioned previously in the literature [17]. However, the superconducting bulk materials became insulating after fired in a furnace in air at a temperature higher than 200 °C for half an hour [18]. Comparatively, by real-time monitoring using the reflection high energy electron diffraction (RHEED) system, we found that it took less than 1 minute for the film diffraction pattern to vanish, when the film was placed in a background pressure  $10^{-4}$  Pa at a temperature higher than 200 °C. There is nothing but some spots remained on the substrate after such a heating process, which can be observed by the naked eyes. The spots are found insulating (The resistance read from a multimeter is in the magnitude of  $M\Omega$ ).

### 3. Superconducting transition in a magnetic field

The in-plane resistance measurement was carried out using the standard four-probe method on one of the  $c$ -axis oriented films grown on STO. Thickness of the film is around 800 Å. The current density used was 700 A/cm<sup>2</sup>. Low ohmic contacts were made to the sample via coating the electrodes with Pt, and using silver paste to attach gold lines to the electrodes firmly.

A part of the  $R - T$  curve measured at zero field is shown in the inset of Fig. 5a. The critical temperature  $T_{Conset}$  is about 47 K with a transition width about 6K (from 90% to 10% of  $\rho_n$ ), which is close to other reports [12, 13, 19]. However, the film has a smaller resistivity just above  $T_C$ ,  $\rho(T|_{T_C}) = 357 \mu\Omega\text{cm}$ . From the graph we can see that the transport behavior is metallic at high temperatures, but at temperatures just above  $T_C$ , the resistance has a very small enhancement. This should not be a contribution from the resistance along  $c$ -axis direction, since in the film  $a$ -axis oriented phase can be fully ruled out according to the XRD data. We would rather attribute the effective enhancement to some kind of weak localizations, although at present we do not have enough evidence to determine what kind of localization it is. We propose that in the film there are some localized charge carriers, so the small enhancement is the combined result of the free carriers itinerating and the localized carriers variable range hopping.

Superconducting transitions of the film in a field of 0.5, 1, 2, 4, 6, 8, and 10 T are presented in Fig. 5a. For a more clear inspection, we plot the H-T phase diagram of the film in Fig. 5b using the criterion 1%, 10%, 50%, 90%, and 99% of  $\rho_n$  respectively. Line 1 is very close to the irreversible line and line 5 is very close to the upper critical field.

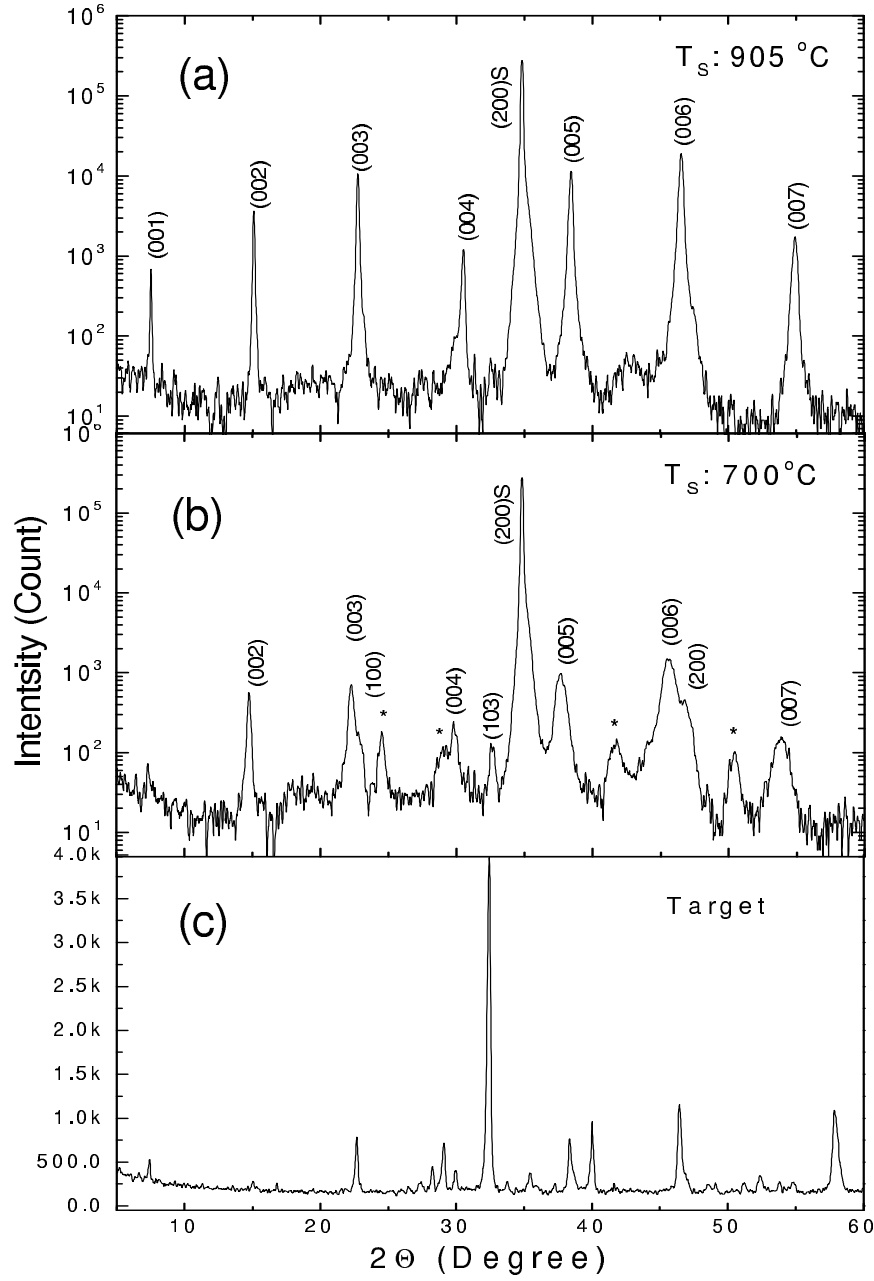


**Figure 3.** Substrate temperature  $T_S$  dependence of the crystal structure for films grown on YSZ. (a) and (b) are the XRD patterns correspond to films grown at  $T_S$  of  $905^\circ\text{C}$  and  $700^\circ\text{C}$ , respectively. Star in (b) denotes the mis-orientation or/and the secondary phase. As a comparison, the XRD pattern of the target is shown in (c).

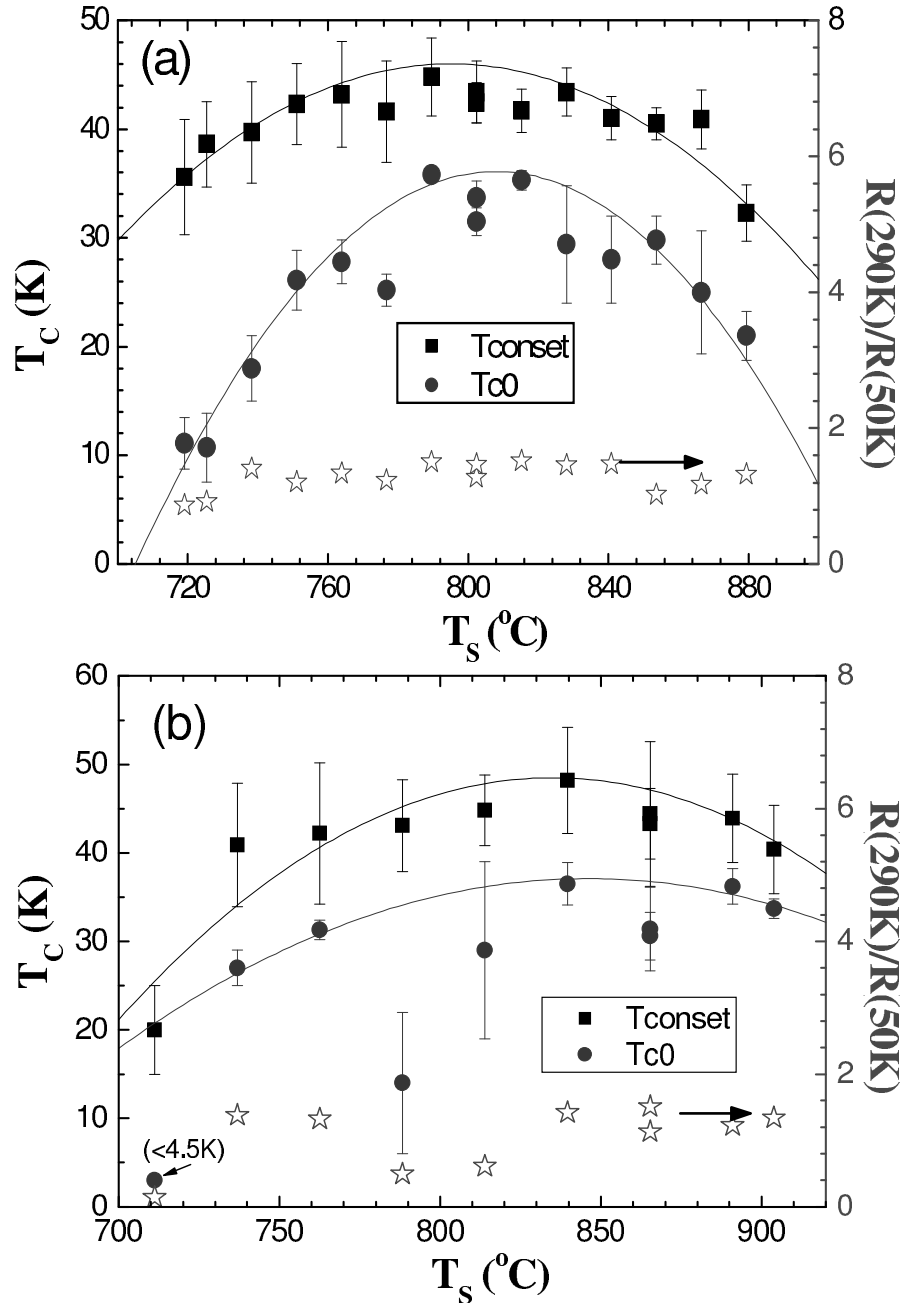


**Figure 4.**  $T_S$  dependence of the superconducting transition temperature  $T_{\text{C0}}$  and  $T_{\text{Conset}}$  for the  $\text{Pr}_{0.5}\text{Ca}_{0.5}\text{Ba}_2\text{Cu}_3\text{O}_{7-\delta}$  films grown on (a) STO and (b) YSZ. Definitions of  $T_{\text{C0}}$  and  $T_{\text{Conset}}$  are detailed in the text. The solid lines in both graphs are just guides to the eyes. The hollow stars represent the ratio  $R(290\text{K})/R(50\text{K})$  in both graphs as directed by the arrow. Thickness of all the films shown here are around  $800\text{\AA}$  for STO and  $1200\text{\AA}$  for YSZ.



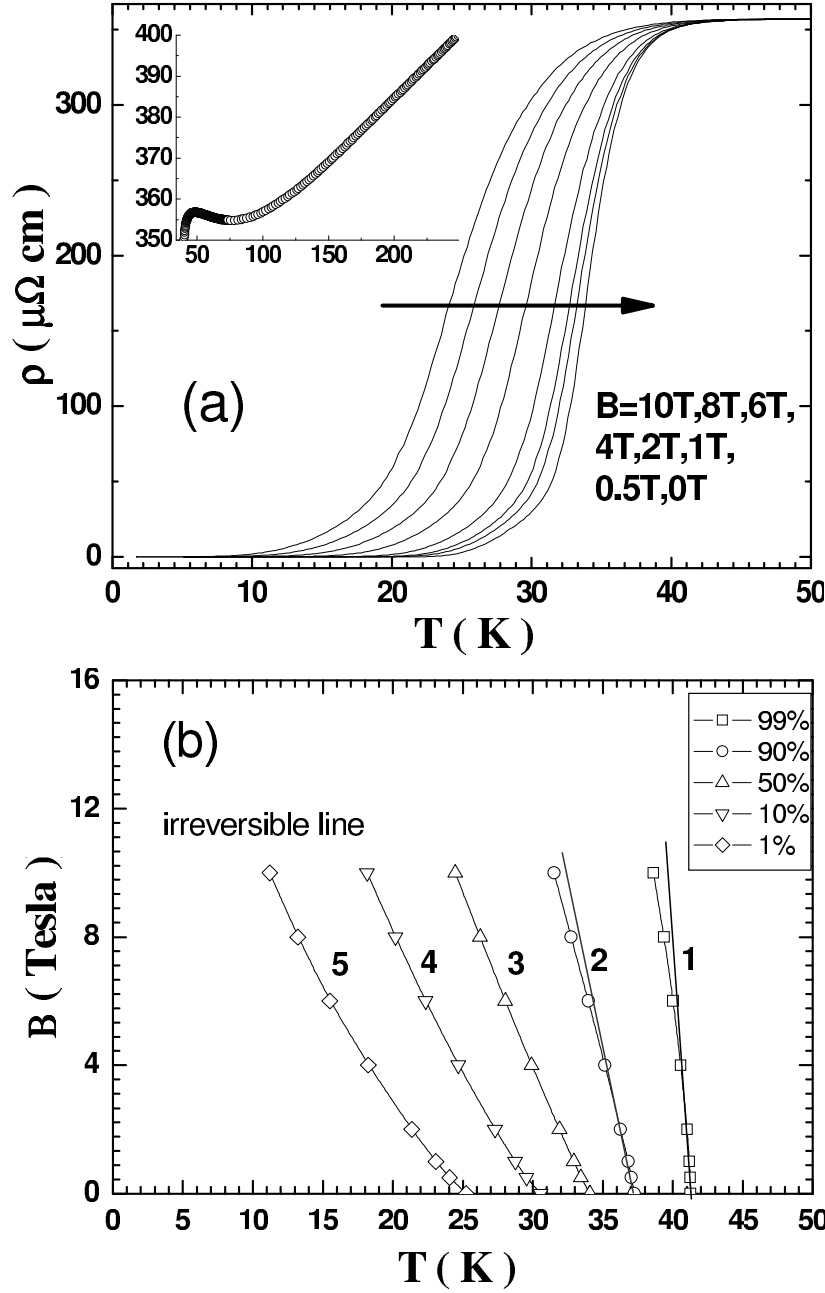


**Figure 5.** (a) Temperature dependence of the film resistivity in various magnetic fields  $H \parallel c$ . A part of the  $R$ - $T$  curve measured at zero magnetic field is shown in the inset. (b)  $H$ - $T$  phase diagram for the epitaxial film at different criterions 1%, 10%, 50%, 90%, and 99% of  $\rho_n$ , corresponding to line 1, 2, 3, 4, 5 respectively.  $B_{C2}(0)$  is estimated using the WHH model to be  $\simeq 105.5$  T and  $\simeq 47.1$  T for line 1 and line 2, respectively. Film thickness here is about 800 Å

#### 4. Discussions

A common feature in the film transport behavior is that the in-plane resistivity ratio  $R(290\text{K})/R(50\text{K})$  is less than 2 (more precisely is 1.6) for the films grown on both STO and YSZ, as indicated by the hollow stars in Fig. 4. Before the superconducting transition, resistivity of these films raises slightly, suggesting a weak carrier localization. The small resistivity slope and the localization-like behavior near the superconducting transition temperature, which are often observed in 50% Pr doped YBCO, are almost independent of the magnetic field strength, as being noticed from the resistivity data at  $B \leq 10$  T. The weak localization behavior could be attributed mainly to the low carrier density, as having been well shown in the underdoped YBCO and  $\text{La}_{1-x}\text{Sr}_x\text{CuO}_4$  systems. In fact, Hall measurements carried out in 50% Ca-doped samples shows an in-plane carrier density lower than that in the optimum-doped YBCO [19, 20]. The weak temperature dependence of normal resistivity indicates an important scattering to the electron from the localized states in the present system. The disorder of Ba and Pr elements could contribute to such localized states, which is possible in the present film grown in an oxygen partial pressure of 40 Pa. The Pr ions may substitute for Ba in the lattice, similar to the Nd and Ba disorder observed in  $\text{Nd}_{1+x}\text{Ba}_{2-x}\text{Cu}_3\text{O}_7$  films grown at oxygen partial pressures higher than 1 bar [21].

So far, it is not well understood why films with a mixed orientation has a better superconductivity than the purely oriented ( $c$  or  $a$ ) films grown on STO. We may attribute this to an improved oxygen intake process for the film of a mixed orientations. In other words, the mobile carrier concentration may be higher in the mixed orientation films than the purely oriented ones, as illustrated by the change of the normal state resistivity slope in Fig.2. Another feature we have noticed is that the small enhancement of the resistivity near  $T_C$  is weakened in the mixed orientation films, and shows a nearly linear temperature dependence of the resistivity as illustrated by the 'mixed oriented' line in Fig.2. And thus seems to suggest an occurrence of structural defects dependent delocalization of the carrier.

We have made an estimate about the upper critical field  $B_{C2}$  from the field-dependent superconducting transition measurements. By using the criterion of the 99% and 90% of the normal-state resistivity  $\rho_n$  for the determination of  $B_{C2}$ , a linear temperature dependence is obtained near  $T_{Conset}$  with a slope  $dB_{C2}/dT$  estimated to be around 3.5 T/K and 1.73 T/K for line 1 and line 2 respectively, as seen in Fig. 5b. Using the Werthamer, Helfand, and Hohenberg (WHH) [22] extrapolation to low temperatures with  $B_{C2}(0) = 0.73(-dB_{C2}/dT|_{T=T_C})T_C$ , the zero-temperature in-plane upper critical field is estimated to be  $B_{C2}^{ab}(0) \simeq 105.5$  T for line 1 and  $B_{C2}^{ab}(0) \simeq 47.1$  T for line 2.

#### 5. Summary

We have grown  $\text{Pr}_{0.5}\text{Ca}_{0.5}\text{Ba}_2\text{Cu}_3\text{O}_{7-\delta}$  epitaxial thin films on different substrates using the pulsed laser ablation technique. Good quality  $a$  and  $c$ -axis oriented films can both be

obtained on STO via varying the substrate temperature. On YSZ, films with good  $c$ -axis orientation have also been grown. The highest  $T_{C0}$  is around 35.6 K and 37 K for films grown on STO and YSZ substrates, respectively. These are consistent with the results of superconductivity in Ca doped  $Pr-123$  as reported by Norton *et al.* previously. The films show a metastable thermostability. The very small  $R(290K)/R(50K)$  ratio together with the localization and a large normal state resistivity of the films is perhaps caused by the essential scattering due to the localized electronic states. The superconducting transitions in a magnetic field up to 10 Tesla for one film grown on STO have been measured. The zero-temperature in-plane upper critical field  $B_{C2}^{ab}(0)$  is also estimated from the resistance data.

## Acknowledgments

We are grateful to G.C. Che for the fruitful discussions. We would also give thanks to S.L. Jia for help in transport property measurements. This work is supported by the National Natural Science Foundation of China (10174093, 10174091, 10221002), the Ministry of Science and Technology of China (NKBRSF-G1999064604) and Chinese Academy of Sciences.

## References

- [1] P.H. Hor, R.L. Meng, Y.Q. Wang, L.Gao, Z.J. Huang, J. Bechtold, K. Forster, and C.W. Chu, *Phys. Rev. Lett.* **58**, 1891 (1987)
- [2] Z. Fisk, J.D. Thompson, E. Zirngiebl, J.L. Smith, and S-W. Cheong, *Solid State Commun.* **62**, 743 (1987)
- [3] L. Soderholm, K. Zhang, D. G. Hinks, M. A. Beno, J. D. Jorgensen, C. U. Segre, and I. K. Schuller, *Nature* **328**, 604 (1987)
- [4] H. A. Blackstead, D. B. Chrisey, J. D. Dow, J. S. Horwitz, A. E. Klanzinger, D. B. Pulling, *Phys. Lett. A* **207**, 109 (1995)
- [5] Z. Zou, J. Ye, K. Oka, Y. Nishihara, *Phys. Rev. Lett.* **80**, 1074 (1998)
- [6] K. Takenaka, Y. Imanaka, K. Tamasaku, T. Ito, and S. Uchida, *Phys. Rev. B* **46**, 5833 (1992)
- [7] B. Fisher, G. Koren, J. Genossar, L. Patlagan, E.L. Gartstein, *Physica C* **176**, 75 (1991); U. Kabasawa, Y. Tarutani, M. Okamoto, T. Fukazawa, A. Tsukamoto, M. Hiratani, K. Takagi, *Phys. Rev. Lett.* **70**, 1700 (1993); B. Fisher, J. Genossar, L. Patlagan, G. M. Reisner, C.K. Subramaniam, A.B. Kaiser, *Phys. Rev. B* **50**, 4118 (1994); W.H. Tang, J. Gao, *Physica C* **315**, 66 (1999)
- [8] M. Akhavan, *Physica B*, **321**, 265-282 (2002)
- [9] A. T. Boothroyd, *J. Alloys Compd.* **303-304**, 489 (2000)
- [10] H.D. Yang, M.W. Lin, C.H. Luo, H.L. Tsay, and T.F. Young, *Physica C* **302**, 320 (1992)
- [11] Y.F. Xiong, Ph.D. Thesis, Institute of Physics, Chinese Academy of Sciences, Beijing (1997)
- [12] D.P. Norton, D.H. Lowndes, B.C. Sales, J.D. Budai, B.C. Chakoumakos, and H.R. Kerchner, *Phys. Rev. Lett.* **66**, 1537 (1991)
- [13] D.P. Norton, D.H. Lowndes, B.C. Sales, J.D. Budai, E.C. Jones, and B.C. Chakoumakos, *Phys. Rev. B* **49**, 4182 (1994)
- [14] Z.X. Zhao, K.Q. Li, and G.C. Che, *Physica C* **341-348**, 331-334 (2000)
- [15] Y.S. Yao, Y.F. Xiong, D. Jin, J.W. Li, F. Wu, J.L. Luo, Z.X. Zhao, *Physica C* **282-287**, 49 (1997)
- [16] M. Luszczek, *Physica C* **355**, 15-22 (2001)
- [17] K.Q. Li, Ph.D. thesis, Institute of Physics, Chinese Academy of Sciences, Beijing (2001)

- [18] Private communications with Prof. G.C. Che.
- [19] Z.H. Wang, Y.F. Sun, G.J. Lian and G.C. Xiong, *Physica C* **341-348**, 2401-2402 (2000)
- [20] J.Y. Xiang *et al.*, unpublished.
- [21] H. Wu, M.J. Kramer, K.W. Dennis, and R.W. McCallum, *Physica C* **290**, 252 (1997)
- [22] N.R. Werthamer, E. Helfand, and P.C. Hohenberg, *Nature* **350**, 596 (1991)